The historic Yangtze River floods: Role of multiscale storm movement

Abstract ID: EGU25-10127

Yixin Yang[1] (yixinyang@smail.nju.edu.cn), Long Yang[1], Gabriele Villarini[2], Ye Shen[1] and Fang Zhao[3]

1-School of Geography and Ocean Science & Frontiers Science Center for Critical Earth Material Cycling, Nanjing University, Jiangsu, China 2-Department of Civil and Environmental Engineering, Princeton University, Princeton, New Jersey, USA 3-School of Geographical Sciences, East China Normal University, Shanghai, China

1. Background

- The Yangtze River Basin (YRB) has repeatedly witnessed devastating, widespread floods.

Table 1. Summary of the most historic widespread floods in YRB over the past century

Year	Q (m^3/s) near the outlet	Socioeconomic impact
1981-2010	60,270	-
1954	92,600	33,000 fatalities, 18.88 million people affected
1998	81,700	1562 fatalities, 84.11 million people affected
2020	83,800	140 fatalities, 6.35 million people affected

- While extensive research has been devoted to understanding the impact of large-scale synoptic conditions and river regulations on these events, the role of storm dynamics has received much less attention.

Research questions

a) What are the causal factors of these widespread floods in terms of atmospheric circulations, storm characteristics and flood propagations?
b) How does widespread flood response depend on multi-scale storm movement?
c) What are the resultant spatiotemporal features of these historic widespread floods?

2. Study area and data

- The YRB is the world third-largest watershed with a total drainage area of 1.8 million km^2.
- Floods in YRB are primarily caused by the movement of summer monsoon rainband.
- The rainfall anomalies are affected by East Asian Summer Monsoon systems including Western Pacific Subtropical High (WPSH) and westerly jet streams.

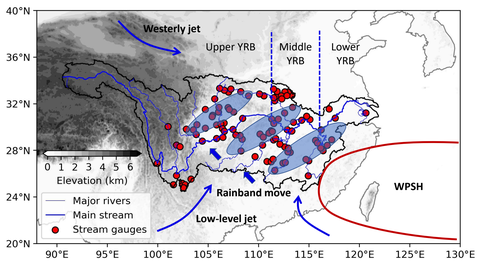

Figure 1. Schematic diagram of atmospheric conditions and flood data distribution

- We conduct comparative analyses among historic widespread floods in the year 1954, 1998 and 2020.
- Our analyses are based on annual maximum flood discharge series from 101 hydrometric stations and daily rain rate from 218 rain gauges.
- We analyze synoptic patterns and rainfall characteristics based on the fifth generation ECMWF reanalysis (ERA5) dataset.

3. Synoptic patterns

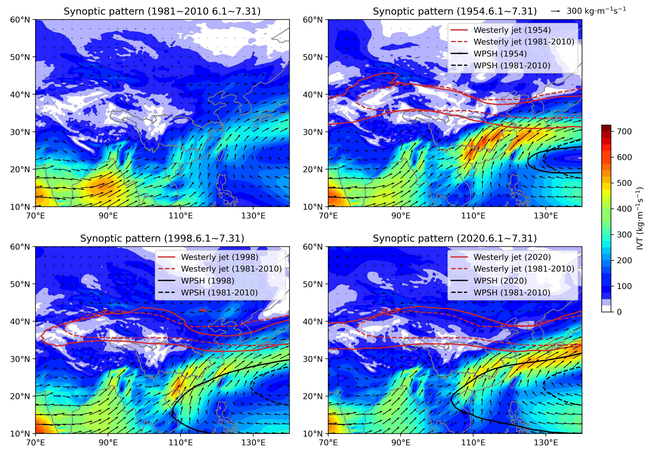

Figure 2. Averaged integrated water vapor transport (IVT) and configuration of key circulation systems

- All the three events are featured by anomalously strong water vapor transport over middle and lower YRB originated from Bay of Bengal.
- The magnitude of IVT of 1954 rank the highest reaching up to twice as the climatology, followed by 2020 and 1998.
- The anomalous wet conditions are associated a westward extension and southward displacement of the WPSH system, and shift of westerly jet towards lower latitudes.

4. Rainfall patterns

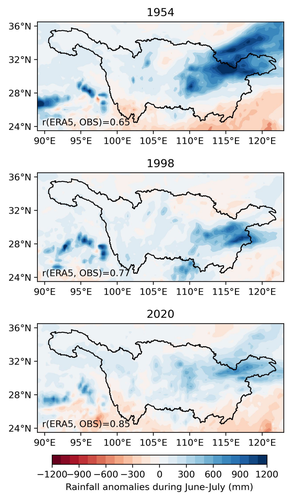

Figure 4. Rainfall anomalies of the three events during Jun.-Jul.

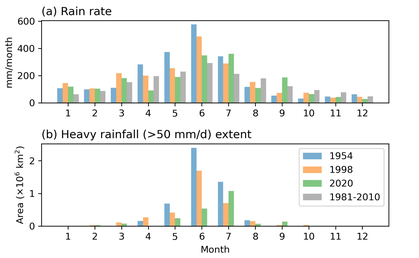

Figure 3. Statistics of rainfall characteristics (110-120°E, 26-32 °N)

- Fig. 3: Widespread and heavy rainfall mainly occur in Jun. and Jul.. The 1954 witnessed the highest antecedent rainfall (970 mm) and Jun.-Jul. accumulated rainfall (917 mm).
- Fig. 4: There are 62%, 73% and 57% of the YRB with positive accumulated rainfall anomalies during Jun.-Jul. 1954, 1998 and 2020, respectively. The heavy rainfall concentrates over middle and lower YRB.
- The ERA5 align well with rainfall observations.

5. Structure and evolution properties of rainband

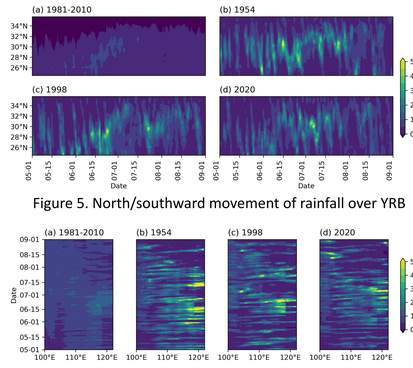

Figure 5. North/southward movement of rainfall over YRB

Figure 6. West/eastward movement of rainfall over YRB

- The rainband of three events show higher spatial variability, coverage and rain rate than the climatology (Fig. 5-6).
- The rainband moves southward in Jun. and Jul. instead of steadily northward as climatology.

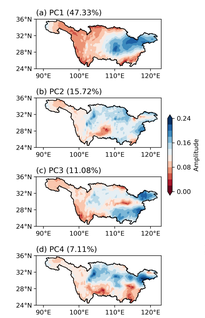

Figure 7. The first four modes of Complex-Empirical Orthogonal Functions (CEOF)

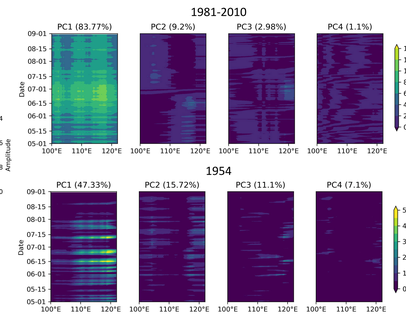

Figure 8. West/eastward movement of the first four modes for climatology (1981-2010, first row) and the year 1954 (second row)

- The rainfall datasets are decomposed into 10 modes based on CEOF, with total explained variance greater than 95%.
- The first mode of rainfall is characterized with a stable location. While the second mode of 1954 demonstrates a continuous sway of double rainbands, distinct from climatology.

6. Interaction of rainfall and drainage systems

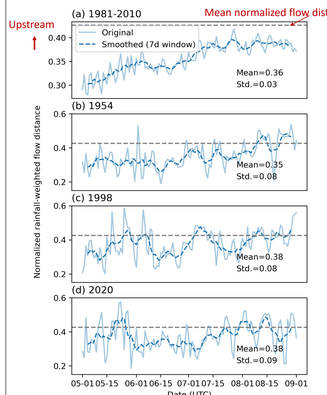

Figure 10. Relative motion of rainband to the drainage network

- The rainbands exhibit more than twice the variability during three historic events compared to the climatological average.
- The three events witnessed rainfall moving downstream over longer period and greater distance.

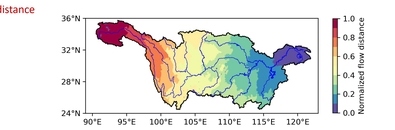

Figure 9. Normalized river distance to the YRB outlet based on flow direction.

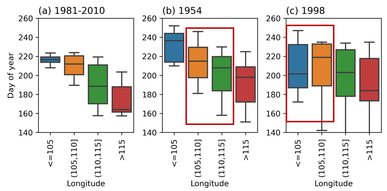

Figure 11. Boxplot of timing of annual maximum flood discharge

- The flood peak timing of the historic events are delayed with greater variability than the climatology.
- The timing around middle reaches are more synchronized for the 1954 flood, and the timing are reversed around upper reaches for the 1998 flood.

7. Summary

- The historic floods over YRB are related to strong water vapor transport originated from the southwest during Jun.-Jul.. This is due to anomalous westward and southward position of the WPSH as well as the southward position of the westerlies.
- The 1954 flood featured by anomalously high antecedent condition and widespread persistent heavy rainfall over middle and lower YRB, ranks the severest over the past century.
- The spatial variability of rainfall for the historic floods is higher than the climatology condition. The rainband swaying across the drainage systems and moving downstream may enhance flood discharge through modulating flood timings.

Abstract information